ORIGINAL RESEARCH

A. Chien
J. Sayre
B. Dong
J. Ye
F. Viñuela

3D Quantitative Evaluation of Atherosclerotic Plaque Based on Rotational Angiography

BACKGROUND AND PURPOSE: Atherosclerosis is a systemic disease that has been shown to cause various cardiovascular diseases and stroke. However, technologies to evaluate the volume of atherosclerotic plaque are limited. We present a method for determination of 3D plaque volume based on RA.

MATERIALS AND METHODS: 3DRA images obtained from patients were used to evaluate the plaque. Six patients who were diagnosed with atherosclerotic lesions were included. The PR model developed for 3DRA was applied to analyze the geometry of the vessel and calculate the plaque volume. To validate the present method, we tested computer-generated phantoms with different degrees of stenosis.

RESULTS: Application of PR to clinical cases allowed the estimation of plaque morphology and quantification of plaque volume. Technique validation showed that on average, PR can rebuild 92% of the plaque and provide satisfactory determination of plaque volume.

CONCLUSIONS: A new approach to obtain plaque volume based on 3DRA is presented. The initial tests in 6 clinical cases and validation with different phantoms showed that this method is feasible. Further validation in a larger clinical series is required to assess the ultimate value of the present technique.

ABBREVIATIONS: ACA = anterior cerebral artery; CPV = computer-estimated plaque volume; ICA = internal carotid artery; MCA = middle cerebral artery; MSR = multiscale representation; PDE = partial differential equation; PR = plaque reconstruction; PV = plaque volume; RA = rotational angiography

Atherosclerosis is a systemic disease that has been shown to cause various cardiovascular diseases and stroke. In particular, atherosclerotic plaque has been associated with many acute clinical complications. Cerebral infarction in the territory of the carotid arteries accounts for most strokes in Western countries and approximately 20% of patients have significant atherosclerotic narrowing at the origin of the internal carotid artery.[1,2] Moreover, approximately 10% of the occurrence of ischemic stroke in the United States is related to intracranial atherosclerotic disease.[3,4] There is an immediate need to assess atherosclerosis in vivo to study the disease.[2,5-8]

Advances in imaging technology have made it possible to observe the 3D geometric changes of blood vessels and evaluate the degree of vessel narrowing in patients by using techniques such as MR imaging and CT.[6,7,9,10] Researchers have also presented various techniques and computational models to assess irregular vascular geometry and to estimate the characteristics of atherosclerotic plaque.[5,7,11-13] While plaque volume has been reported as an important tool for patient management and for evaluating new therapies,[14-16] methods to evaluate this index are limited.[14,15,17,18] Because conventional angiography remains the criterion standard for the diagnosis of vascular diseases,[19,20] techniques that can quantify plaque by using conventional angiography data can be useful.

In this article, we present a technique, PR, to quantify atherosclerotic plaque volume from 3DRA. On the basis of the concept of MSR,[21,22] we developed the PR model to recover the vessel lumen at the regions of the atherosclerotic lesions and to compute the morphology of the plaque. Because different volumes of plaque may relate to different clinical risks, to verify that the proposed method is accurate and useful for ranges of atherosclerotic conditions, we tested and validated phantoms with various degrees of stenosis. Our initial experiences with PR in patients showed that this method can compute plaque in different arteries.

Received July 14, 2010; accepted after revision October 15.

From the Division of Interventional Neuroradiology (A.C., F.V.), David Geffen School of Medicine at UCLA; Department of Biostatistics (J.S.), School of Public Health; and Department of Mathematics (B.D., J.Y.), UCLA, Los Angeles, California.

Please address correspondence to Aichi Chien, PhD, Division of Interventional Neuroradiology, David Geffen School of Medicine at UCLA, 10833 LeConte Ave, Box 951721, Los Angeles, CA 90095; e-mail: aichi@ucla.edu

DOI 10.3174/ajnr.A2483

Materials and Methods

Case Selection and Imaging

Patients who were diagnosed with atherosclerosis were selected from the clinical data bases at the Division of Interventional Neuroradiology, UCLA Medical Center from 2009 to 2010. Among these patients (total of 10), 7 had 3DRA imaging of the atherosclerotic regions. One patient was excluded due to inadequate image quality for 3D reconstruction. At the end, 6 patients were selected. The locations of the atherosclerosis were the following: cases I and IV, the ACA; cases II and V, the MCA; and cases III and VI, the ICA. The 3D rotational cerebral angiograms were acquired with an Integris unit (Philips Healthcare, Best, the Netherlands). To perform the plaque computation, we transferred the 3D data to a Dell 490 workstation for the mathematic modeling and reconstruction of the plaque.

Mathematic Modeling and Reconstruction of Atherosclerotic Plaque

Angiography captures contrast injected into the blood stream, and it is the vessel lumen that is imaged. Regions of irregular lumen in angiographic images, such as local narrowing and lack of contrast (Fig 1*A*), are an important indication of vascular diseases.[2,5] Our technique to compute the plaque is the following: First denote these geo-

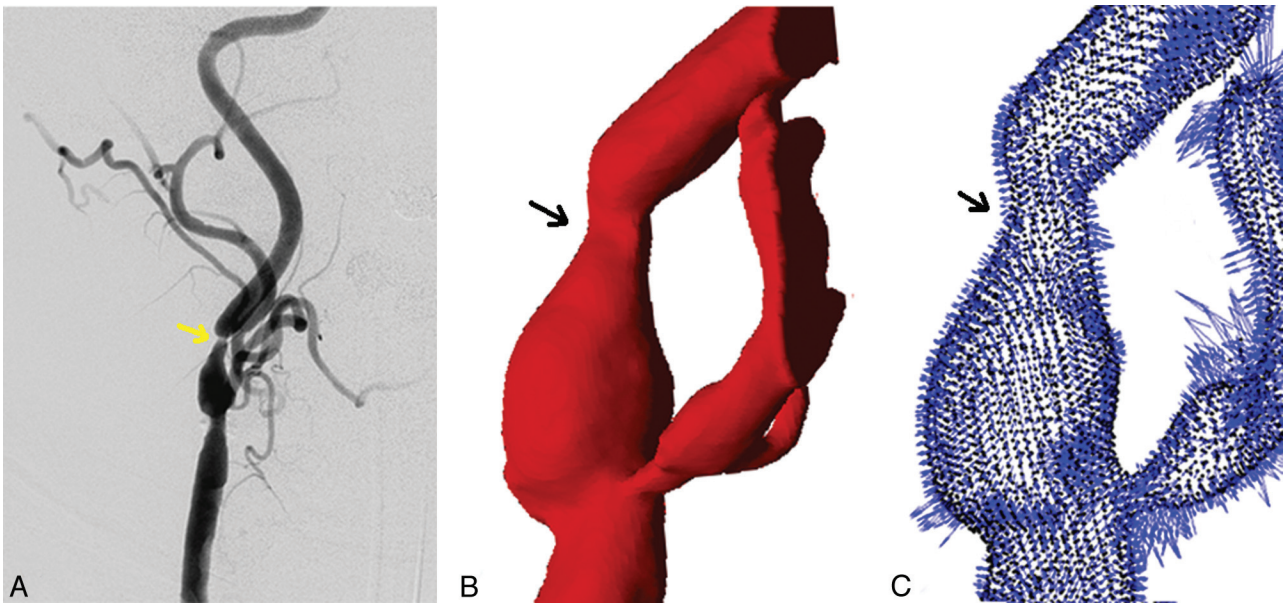

Fig 1. Representative angiographic images indicating the location of atherosclerotic plaque (*yellow arrow, A*) and 3D reconstruction of the same blood vessel (*B*) in mathematic indices ready for the plaque-estimation algorithm vector field (*C*), which encodes surface curvature.

metric changes with numeric indices and then extract curvature parameters to find the smooth-vessel wall.

In the PR model, the vessel geometry was first transformed into a mathematic expression (Appendix A) based on the MSR for shapes (Fig 1).[21,22] It allowed the representation of vessel geometries as a sequence of multiscaled detailed features by using level set motions.[23] Then, we implemented the fast diffusion-generated motion algorithm in the numeric procedure to solve the Hamilton-Jacobi–like equations.[24] Through the MSR, we separated the vessel detail from the smooth components of the vessel. These features were later incorporated to facilitate an accurate reconstruction of the given vessel near the atherosclerotic lesion. Finally, the vessel was recovered by filling in the data on the basis of the surrounding geometry, such as surface curvatures (Fig 1*C*).[25,26] At the end, by taking the difference between the reconstructed vessel and the original vessel, we could estimate the volume of plaque. Mathematic formulations and computer algorithms for the PR model are summarized in Appendices A–C.

Technique Validation

To validate the PR algorithm, we used computer-generated phantoms created by using Matlab (MathWorks, Natick, Massachusetts) to simulate various scenarios of stenosis. Phantoms were made to represent vessels 20 mm in length and 5 mm in lumen diameter. We tested unilateral and bilateral plaque phantoms with stenoses of 30%, 60%, and 90%. For each degree of stenosis, experiments of different ranges of atherosclerotic lesions (5, 10, and 15 mm) in the direction of the vessel long axis were performed.

Statistical Analysis

The Wilcoxon signed rank tests were performed to analyze the results of PR. The statistical significance level was set at .05.

Results

Reconstructions of atherosclerotic plaque are shown in Fig 2 for cases I, II, and III and Fig 3 for cases IV, V, and VI. From the left to right are lesions at the ACA (Figs 2*A* and 3*A*), MCA (Figs 2*B* and 3*B*), and ICA (Figs 2*C* and 3*C*). The top row is the diagnostic angiogram showing the atherosclerotic lesion. The second row is 3D geometry of the vessel built with RA images. The third row shows the reconstruction of the plaque for each case (yellow) and the percentage of flow obstruction by the plaque. At the bottom, the plaque subtracted from the blood vessel is presented, displaying the morphology and volume of the plaque.

Technique Validation

Representative phantoms with different degrees of stenosis are shown in Fig 4*A*. Phantoms with a smooth cylindric vessel (Fig 4*B*) represent healthy vessels without atherosclerotic disease. To validate the plaque quantification, we compared the CPV against the PV found by taking the difference between the healthy vessel and the vessel with stenosis. The ratio of CPV to PV for each phantom (CPV/PV) is shown in Fig 4*C*.

We tested cases with the plaque formed unilaterally and bilaterally with 30%, 60%, and 90% stenoses. Different lesion sizes (5, 10, and 15 mm) along the vessel axis were also included to evaluate whether PR is robust for different plaque sizes. Figure 4*C* shows the representative reconstruction of plaques in unilateral (left) and bilateral (right) phantoms. For the unilateral cases, on average, 92.8% of plaque (CPV/PV = 92.8%) was successfully reconstructed. There was no statistical difference between CPV and PV for 30%, 60%, and 90% unilateral stenoses ($P = .109$, $P = .285$, and $P = .593$, respectively). For the bilateral atherosclerotic cases, on average, 91.5% of plaque (CPV/PV = 91.5%) was successfully reconstructed. There was no statistical difference between CPV and PV for 30%, 60%, and 90% bilateral stenoses ($P = .083$, $P = .109$, and $P = .109$, respectively). Overall, PR was able to reconstruct 92.2% of plaque.

Discussion

Conventional angiography is the standard diagnostic tool for intracranial atherosclerosis, which is often found as luminal irregularity in the angiogram, and it is assumed that the plaque

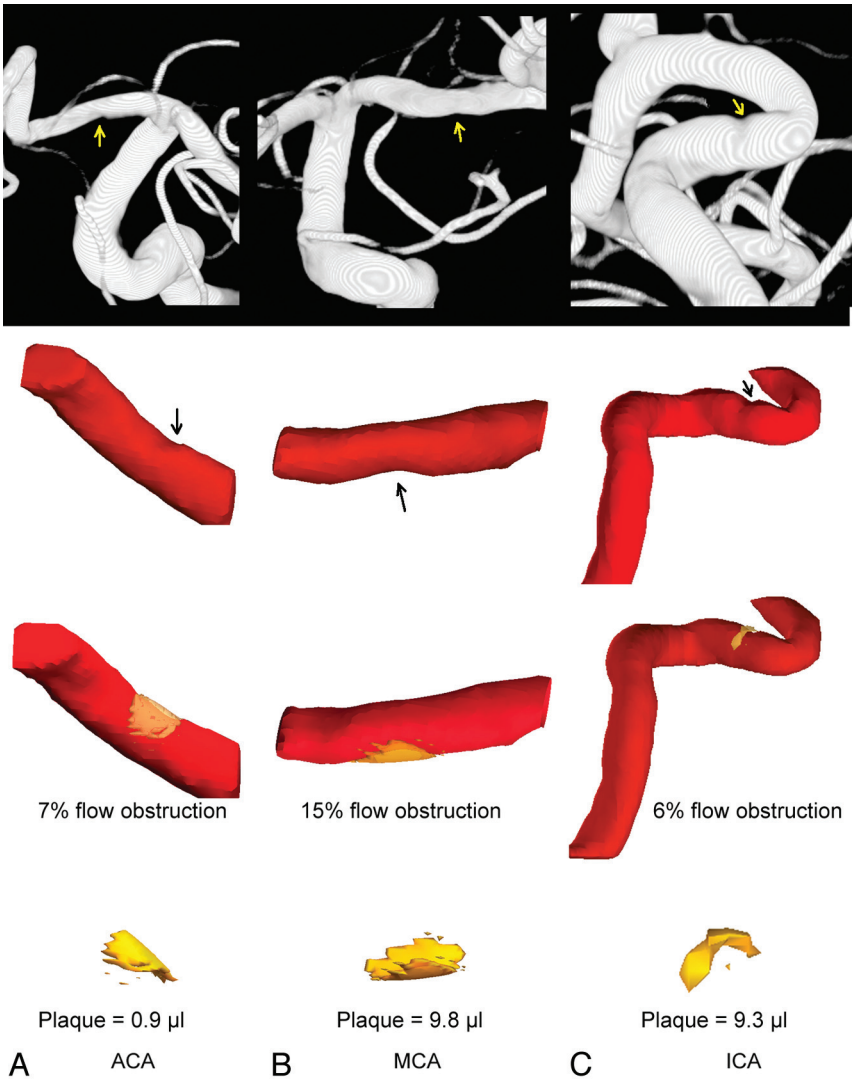

Fig 2. Plaque quantification for cases I the ACA (*A*), II the MCA (*B*), and III the ICA (*C*). The top row is the diagnostic images with arrows indicating stenosis. The second row shows the 3D geometry of the vessel built with 3DRA images with arrows indicating stenosis. The third row shows the reconstructed plaque (yellow) and the percentage of flow obstruction computed by the program. The bottom row shows the morphology and volume of the plaque in units of microliters.

lining the vessel wall results in such irregularity.[19,20,27] The purpose of this study was to develop a technique that can evaluate the volume of plaque by using conventional angiography. We introduced the PR model to reconstruct plaque on the basis of MSR principles that have been applied to study various biologic shapes.[21,22]

There has been much effort to develop evaluation criteria and measurement methods to study atherosclerotic plaque.[28,29] Researchers have shown that the plaque volume can be a reliable measure for studying atherosclerosis.[14,30] A recent randomized trial also used this quantity as 1 of the indices to track the plaque changes with time.[16] Therefore, there is considerable value in quantifying the plaque volume from 3D angiograms. Our preliminary results showed that using PR to assess plaque volume is feasible for clinical images. Because an atherosclerotic lesion is often diagnosed or verified with catheter angiograms, this technique can help to estimate the morphology and volume of the plaque and to study the disease.

In the technique validation, we performed tests by using phantoms with different degrees of stenosis. The results showed that the algorithms allow the reconstruction of plaque in different scenarios. On average, 92% of the plaque can be rebuilt through the proposed method, regardless of the lesion size. Additional effort such as implementing advanced computation schemes can be helpful to improve the CPV/PV ratio of the current model. Furthermore, research using postsurgical specimens to validate the plaque volume estimation is essential to understand the accuracy of the present method.

Conclusions

We present a new approach to estimate the volume of atherosclerotic plaque on the basis of 3DRA. Analysis and validation with different phantoms to simulate various degrees of stenosis have shown that this method provides satisfactory volume computation. The initial results of the clinical application suggest that this method is feasible. Further validation in a larger clinical series is required to assess the ultimate value of the present technique.

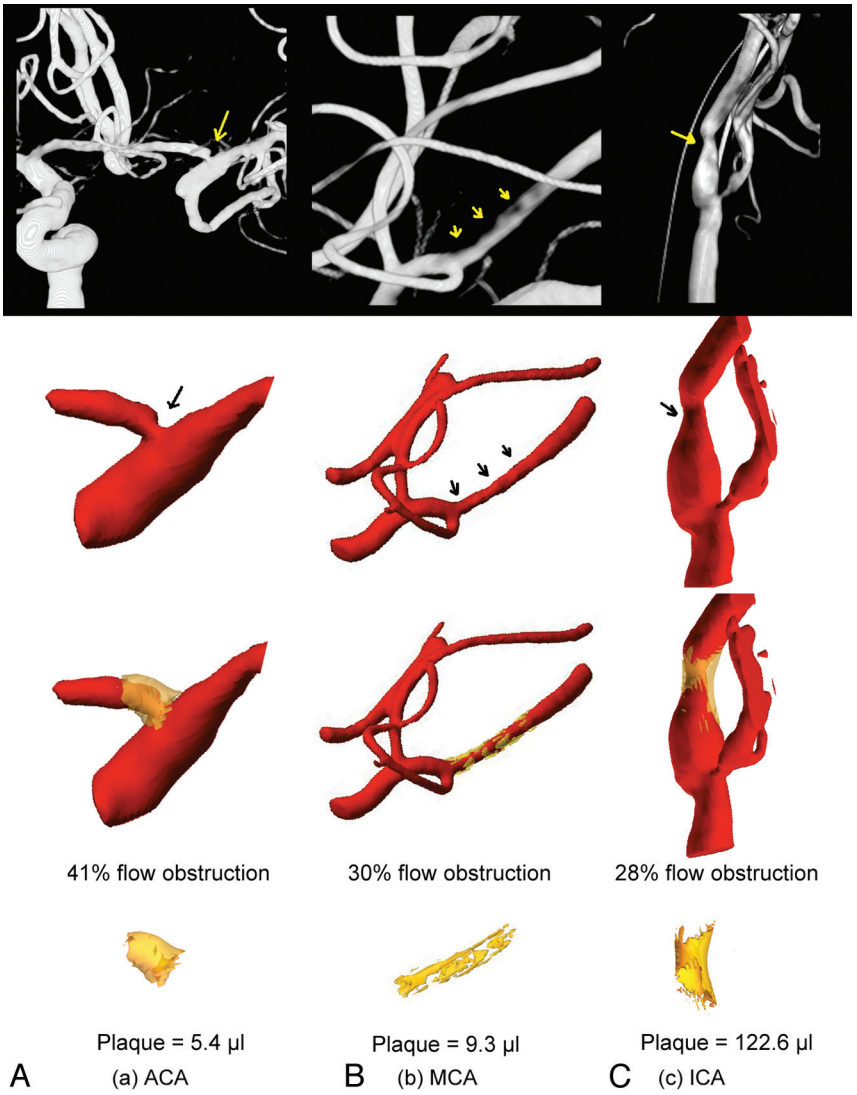

Fig 3. Plaque quantification for cases IV the ACA (*A*), V the MCA (*B*), and VI the ICA (*C*). The top row is the diagnostic images with arrows indicating stenosis. The second row shows the 3D geometry of the vessel built with 3DRA images and arrows indicating stenosis. The third row shows the reconstructed plaque (yellow) and the percentage of flow obstruction. The bottom row shows the morphology and volume of the plaque in units of microliters.

Appendix

A) Vessel Lumen Geometry

We first reconstructed the blood vessel lumen and expressed boundaries ∂D of domains $D \in \mathbb{R}^3$ by level set functions[23] ϕ as the following:

$$1) \qquad \phi(x)\begin{cases} < 0, & x \in D \\ > 0, & x \in D^c \end{cases}$$

The multiscale representation of a blood vessel then can be obtained by level set motions through the following Hamilton-Jacobi–like equation:

$$2) \qquad \phi_t + v_n(\nabla\phi)|\nabla\phi| = 0, \quad \phi(x, 0) = \phi_0(x),$$

where ϕ_0 is the level set function of the given blood vessel, v_n is the velocity field, and $t \in [0, T]$. To obtain a second-order approximation to PDE (equation 2) and reduce the complexity of solving the nonlinear PDE, the diffusion-generated motion technique was used to solve PDE (equation 2).[24] Therefore, the continuous transform of the vessel ϕ_0, and its inverse transform can be expressed as equations 3 and 4 respectively with $\phi(x, t)$, the solution of PDE (equation 2):

$$3) \qquad W(\phi_0) := \overrightarrow{W}(x, t) := -v_n\frac{\nabla\phi}{|\nabla\phi|}$$

$$4) \qquad \psi_t + \overrightarrow{W}(x, t)\cdot\nabla\psi = 0, \quad \psi(x, 0) = \phi(x, T).$$

Then, we denote $\overrightarrow{W}_1(x, t)$ as the restriction of $\overrightarrow{W}(x, t)$ on $S_t := \{x: \phi(x, t)=0\}$, and express an MSR for the original vessel S_o as equation 5, which is invariant under rigid-body transformation and initial embeddings of ϕ_0:

$$5) \qquad MSR(S_0) = \{\{\overrightarrow{W}_1(x, t)\}_{t\in[0, T]}, S_0\},$$

B) Reconstruction of Atherosclerotic Plaque

We used MSR as described above for the geometric representations of the blood vessel, where we chose the normal-velocity field in PDE (equation 2) to be $v_n = c + \kappa_a - \kappa$ (Fig 1*C*). κ and κ_a are the mean curvature and average mean curvature, respectively. c is constant. After solving PDE (equation 2)[24],

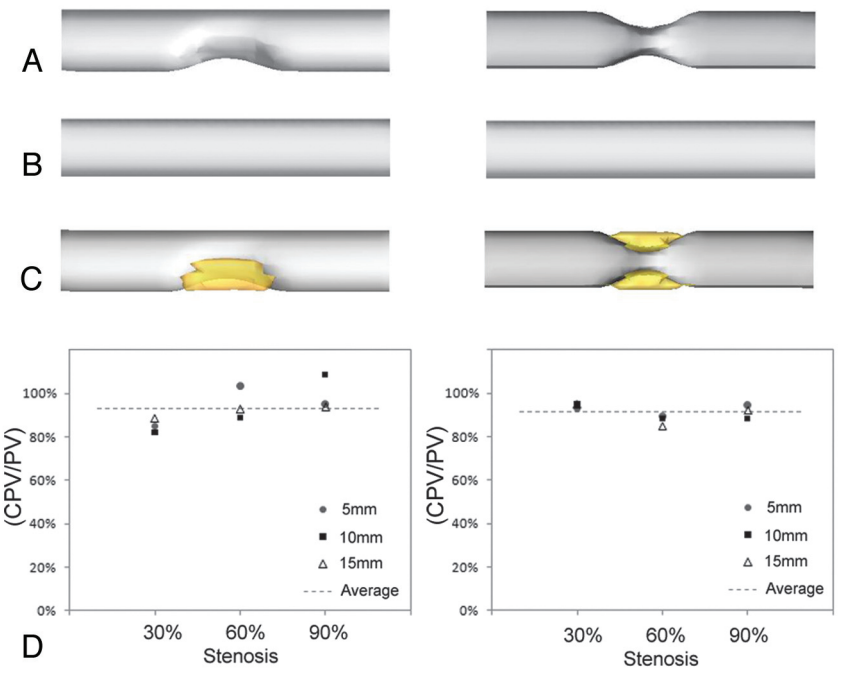

Fig 4. *A,* Representative unilateral (left) and bilateral (right) stenosis phantoms. *B,* The ideal vessel without stenosis. *C,* The reconstructed plaque for the unilateral (left) and bilateral (right) models. *D,* The percentage of the volume estimation (CPV/PV) for lesion sizes 5, 10, and 15 mm in the direction of the vessel long axis.

we recorded the details $\overrightarrow{W}(x, t)$ for all x in a narrow band of $\phi(x, t)$. This step is crucial to ensure that the reconstruction is accurate. Finally, the vessel was reconstructed with $\psi_t + \overrightarrow{W}(x, t) \cdot \nabla\psi = \epsilon\nabla_2\psi$, where ϵ is diminished for each iteration. When ϵ goes to zero, the solution will converge to the solution of equation 4. Therefore, a diminishing ϵ ensures the final convergence of our calculation.

C) Summary of Algorithms to Reconstruct Atherosclerotic Plaques

1) Perform MSR transform of the given vessel by solving PDE (2) with

$$v_n = c + \kappa_a - \kappa,$$

by using the fast diffusion-based level set motion.

2) Record the details $\overrightarrow{W}(x,t)$ for all x in a narrow band of $\phi(x, t)$.

3) Reconstruct the blood vessel through the following equations:

$$\psi_i + \overrightarrow{W}(x, t) \cdot \nabla\psi = \epsilon\nabla^2\psi, \quad \psi(x, 0) = \phi(x, T).$$

4) Apply the data outside the inpainting domain and repeat until the level set function satisfies the following equation:

$$\| \phi\ current(x,0) - \phi\ previous(x,0) \| < 0.01$$

Disclosures: James Sayre. *Research Support (including provision of equipment or materials):* UCLA Department of Radiological Sciences.

References

1. Harrison MJ, Marshall J. **Prognostic significance of severity of carotid atheroma in early manifestations of cerebrovascular disease.** *Stroke* 1982;13:567–69
2. Rothwell PM, Gibson R, Warlow CP. **Interrelation between plaque surface morphology and degree of stenosis on carotid angiograms and the risk of ischemic stroke in patients with symptomatic carotid stenosis: on behalf of the European Carotid Surgery Trialists' Collaborative Group.** *Stroke* 2000;31:615–21
3. Sacco RL, Kargman DE, Gu Q, et al. **Race-ethnicity and determinants of intracranial atherosclerotic cerebral infarction: the Northern Manhattan Stroke Study.** *Stroke* 1995;26:14–20
4. Chimowitz MI, Kokkinos J, Strong J, et al. **The Warfarin-Aspirin Symptomatic Intracranial Disease Study.** *Neurology* 1995;45:1488–93
5. Troyer A, Saloner D, Pan XM, et al. **Major carotid plaque surface irregularities correlate with neurologic symptoms.** *J Vasc Surg* 2002;35:741–47
6. Wyers MC, Powell RJ, Fillinger MF, et al. **The value of 3D-CT angiographic assessment prior to carotid stenting.** *J Vasc Surg* 2009;49:614–22
7. Ryu CW, Jahng GH, Kim EJ, et al. **High resolution wall and lumen MRI of the middle cerebral arteries at 3 Tesla.** *Cerebrovasc Dis* 2009;27:433–42
8. Lewis SJ. **Prevention and treatment of atherosclerosis: a practitioner's guide for 2008.** *Am J Med* 2009;122:S38–50
9. Phan T, Huston J 3rd, Bernstein MA, et al. **Contrast-enhanced magnetic resonance angiography of the cervical vessels: experience with 422 patients.** *Stroke* 2001;32:2282–86
10. Feldmann E, Wilterdink JL, Kosinski A, et al. **The Stroke Outcomes and Neuroimaging of Intracranial Atherosclerosis (SONIA) trial.** *Neurology* 2007;68:2099–106
11. Saam T, Ferguson MS, Yarnykh VL, et al. **Quantitative evaluation of carotid plaque composition by in vivo MRI.** *Arterioscler Thromb Vasc Biol* 2005;25:234–39
12. Becker CR. **Assessment of coronary arteries with CT.** *Radiol Clin North Am* 2002;40:773–82
13. Nahrendorf M, Keliher E, Panizzi P, et al. **18F–4V for PET-CT imaging of VCAM-1 expression in atherosclerosis.** *JACC Cardiovasc Imaging* 2009;2:1213–22
14. Spence JD. **Technology insight: ultrasound measurement of carotid plaque—patient management, genetic research, and therapy evaluation.** *Nat Clin Pract Neurol* 2006;2:611–19
15. de Labriolle A, Mohty D, Pacouret G, et al. **Comparison of degree of stenosis and plaque volume for the assessment of carotid atherosclerosis using 2-D ultrasound.** *Ultrasound Med Biol* 2009;35:1436–42
16. Stumpe KO, Agabiti-Rosei E, Zielinski T, et al. **Carotid intima-media thickness and plaque volume changes following 2-year angiotensin II-receptor blockade: the Multicentre Olmesartan Atherosclerosis Regression Evaluation (MORE) study.** *Ther Adv Cardiovasc Dis* 2007;1:97–106
17. Brodoefel H, Burgstahler C, Sabir A, et al. **Coronary plaque quantification by voxel analysis: dual-source MDCT angiography versus intravascular sonography.** *AJR Am J Roentgenol* 2009;192:W84–89
18. Isbell DC, Meyer CH, Rogers WJ, et al. **Reproducibility and reliability of atherosclerotic plaque volume measurements in peripheral arterial disease with cardiovascular magnetic resonance.** *J Cardiovasc Magn Reson* 2007;9:71–76

19. **Quality improvement guidelines for adult diagnostic neuroangiography: cooperative study between the ASNR, ASITN, and the SCVIR—American Society of Neuroradiology. American Society of Interventional and Therapeutic Neuroradiology. Society of Cardiovascular and Interventional Radiology.** *AJNR Am J Neuroradiol* 2000;21:146–50
20. Easton JD, Saver JL, Albers GW, et al. **Definition and evaluation of transient ischemic attack: a scientific statement for healthcare professionals from the American Heart Association/American Stroke Association Stroke Council—Council on Cardiovascular Surgery and Anesthesia; Council on Cardiovascular Radiology and Intervention; Council on Cardiovascular Nursing; and the Interdisciplinary Council on Peripheral Vascular Disease. The American Academy of Neurology affirms the value of this statement as an educational tool for neurologists.** *Stroke* 2009;40:2276–93. Epub 2009 May 7
21. Nain D, Haker S, Bobick A, et al. **Multiscale 3D shape analysis using spherical wavelets**. *Med Image Comput Comput Assist Interv* 2005;8(pt 2):459–67
22. Pauly M, Kobbelt L, Gross M. **Point-based multiscale surface representation.** *ACM Trans Graph* 2006;25:177–93
23. Osher SJ, Fedkiw RP. *Level Set Methods and Dynamic Implicit Surfaces.* New York: Springer-Verlag; 2003
24. Esedoglu S, Ruuth S, Tsai R. **Diffusion generated motion using signed distance functions**. *J Comput Phys* 2010;229:1017–42
25. Antiga L, Ene-Iordache B, Remuzzi A. **Computational geometry for patient-specific reconstruction and meshing of blood vessels from MR and CT angiography.** *IEEE Trans Med Imaging* 2003;22:674–84
26. Verdera J, Caselles V, Bertalmio M, et al. **Inpainting surface holes**. In: *Proceedings of the International Conference on Image Processing,* Barcelona, Catalonia, Spain. September 14–17, 2003
27. Loh Y, Duckwiler GR. **Extracranial stenosis: endovascular treatment**. *Neuroimaging Clin N Am* 2007;17:325–36, viii
28. Eliasziw M, Rankin RN, Fox AJ, et al. **Accuracy and prognostic consequences of ultrasonography in identifying severe carotid artery stenosis: North American Symptomatic Carotid Endarterectomy Trial (NASCET) Group.** *Stroke* 1995;26:1747–52
29. Rothwell PM, Gibson RJ, Slattery J, et al. **Equivalence of measurements of carotid stenosis: a comparison of three methods on 1001 angiograms—European Carotid Surgery Trialists' Collaborative Group.** *Stroke* 1994;25:2435–39
30. Landry A, Spence JD, Fenster A. **Measurement of carotid plaque volume by 3-dimensional ultrasound.** *Stroke* 2004;35:864–69